TITLE

Proof of concept study deploying CRISPR inhibition and activation opens new avenues for systematic biological exploration in zebrafish.

AUTHORS

Nelson B. Barrientos[1], Elyse A. Shoppell[1], Rachel J. Boyd[1], Valeria C. Culotta[2], Andrew S. McCallion[1,3*]

AFFILIATIONS

[1]McKusick-Nathans Department of Genetic Medicine, Johns Hopkins University School of Medicine, Baltimore, MD 21205, USA

[2]Department of Biochemistry and Molecular Biology, Johns Hopkins University Bloomberg School of Public Health, Baltimore, MD 21205, USA

[3]Department of Medicine, Johns Hopkins University School of Medicine, Baltimore, MD 21205, USA

[*] Corresponding author

Corresponding author's email: andy@jhmi.edu

ABSTRACT

The application of CRISPR interference (CRISPRi) and CRISPR activation (CRISPRa) technologies in zebrafish has the potential to expand its capacity for the study of gene function significantly. We report proof-of-principle data evaluating transient expression of a codon optimized CRISPRi/a system for zebrafish across established pigmentary and growth phenotypes. A codon-optimized and catalytically inactive *cas9* gene (*dcas9*) was cloned upstream of codon-optimized Krüppel associated box (KRAB) and methyl-CpG binding protein 2 (MeCP2) for CRISPRi, and VP64 for CRISPRa. To validate CRISPRi, we targeted key genes in melanocyte differentiation (*sox10* and *mitfa)*; and melanin production (tyrosinase; *tyr*). Microinjection of CRISPRi mRNA and single guide RNAs (sgRNAs) targeting the *tyr* promoter or 5'-UTR resulted in larvae with hypopigmented epidermal melanocytes. Similarly, CRISPRi targeting of the *sox10 or mitfa* promoters results in hypopigmentation of epidermal melanocytes consistent with their roles upstream of *tyr,* and the role of *sox10* in activation of *mitfa*. Finally, we tested both CRISPRi/a to modulate a single gene to yield hypomorphic and hypermorphic effects, selecting *mrap2a* as our target. This gene regulates energy homeostasis and somatic growth via inhibition of the melanocortin 4 receptor gene (*mc4r*). We show that inactivating or activating *mrap2a* with CRISPRi/a significantly decreases or increases larval body length, respectively. We demonstrate that CRISPRi/a can modulate control of zebrafish gene expression, facilitating efficient assay of candidate gene function and disease relevance.

KEYWORDS:

Zebrafish, CRISPR-activation, CRISPR-inhibition

INTRODUCTION

Zebrafish (*danio rerio*) are a powerful model system in which to study functional components of vertebrate genomes. Comparative genomics analyses have shown that 61.5% of mouse protein-coding genes and 71% of human protein-coding genes have at least one zebrafish orthologue (1,2). Additional features, including short generation time, high fecundity, external fertilization, and embryonic transparency, have distinguished zebrafish as a desirable model system in which to examine developmental processes. As such, zebrafish have been widely used to study the biological relevance of regulatory elements (3–6), and human disease-associated genes (7–14).

Emerging technologies for transgenesis and genome engineering, such as such as Gal4-UAS (15); Tol2-transposase transgenesis (3); Zinc Finger Nucleases (16); and transcription activator-like effectors (TALENs) (17) have been developed and rapidly implemented in zebrafish. Over the last decade, zebrafish have also been shown to be amenable to CRISPR-Cas-based genomic engineering applications, including targeted mutagenesis, base editing, and generation of knock-in and knockout models (18–22). More recently, the emergence of CRISPR interference (CRISPRi) and activation (CRISPRa) have presented additional opportunities to explore functional components of vertebrate genomes. CRISPRi/a involves the fusion of transcriptional effectors to a catalytically inactive, or “dead” Cas9 (dCas9). CRISPRi employs a transcriptional repressor, such as a Krüppel associated box (KRAB) domain and methyl-CpG binding protein 2 (MeCP2) (23,24), while in the case of CRISPRa, a transcriptional activator, such as VP64, is fused to the dCas9 (25). To date, the CRISPRi/a systems have seen limited application in zebrafish (26), whereas they have been more rapidly employed in mammalian organisms to target human disease-relevant genes (27–29).

Here, we report initial experiments in the development and evaluation of zebrafish codon-optimized zdCas9-KRAB-MeCP2 and zdCas9-VP64 CRISPR systems. We present a systematic

evaluation of these modified proteins in functional proof-of-concept experiments by targeting two easily scored phenotypes: zebrafish pigmentation and somatic growth. In addition to providing visual confirmation of the efficacy of both CRISPRi and CRISPRa, these two model phenotypes and their corresponding pathways are well-characterized and are involved in human disease.

Specifically, we chose to test our CRISPRi system by targeting genes involved in melanocyte differentiation and pigmentation, *sox10 (SRY*-box transcription factor 10*)*, *mitfa* (melanocyte inducing transcription factor a), and the gene for the rate-determining enzyme in pigmentation, *tyr (*tyrosinase*)*. *sox10* directly activates the *mitfa* promoter to stimulate downstream genes involved in melanocyte differentiation (33,34); this leads to the activation of *tyr*, at approximately 16 hours post fertilization (16 hpf) to induce melanin production by 24 hpf (30–32). In the developing zebrafish embryo, due to whole-genome duplication, *mitfa* is co-expressed with *mitfb* in the retinal pigment epithelium, but only *mitfa* is expressed in neural crest cells, which differentiate to give rise to epidermal melanocytes (31,33,34).

We hypothesize that independently targeting each of these genes with functional CRISPRi will yield a visible reduction in zebrafish pigmentation. In the case of *sox10,* we expect to see marked reduction in pigmentation globally due to its role in melanocyte cell fate and activation of *mitfa* and *tyr* to promote melanin production in zebrafish and other vertebrates (35,36). Due to its role in multiple stages of melanocyte differentiation and its function as a transcription factor, silencing *mitfa* is also expected to result in phenotype of epidermal hypopigmentation (37,38). Lastly, we hypothesize that targeting the rate-determining enzyme in melanin pigment formation (*tyr)* will result in hypopigmentation of melanocytes throughout the zebrafish body (30,35,39,40). Zebrafish melanocytes have been extensively studied by our group and others (4,6,41,42), and targeting genes in this pathway is highly relevant to the study of human disease, including melanoma (43–45), Waardenburg Syndrome (46,47), microphthalmia, and Hirschsprung's disease (48,49).

99 Expanding from this initial study, we sought to apply both CRISPRi and CRISPRa to
100 *mrap2a*, a gene with known inhibitory activity to regulate somatic growth in the zebrafish embryo
101 (50). *mrap2a* encodes the melanocortin receptor accessory protein 2a, which has been found to
102 inhibit the transcription of the *mc4r* (melanocortin-4 receptor) (50). We hypothesize that targeting
103 the *mrap2a* promoter with CRISPRa will increase *mrap2a* expression and therefore amplify the
104 inhibition of *mc4r* and promote visible overgrowth phenotypes in zebrafish larvae. This is
105 supported by evidence in human patients, wherein autosomal dominant loss of function mutations
106 in *MCR4* results in severe childhood-onset obesity (51,52). By contrast, we hypothesize that
107 effective CRISPRi targeting of *mrap2a* will result in decreased *mc4r* inhibition and result in
108 undergrown zebrafish larvae, consistent with reported morpholino-based knock-down
109 experiments (50).

110 Ultimately, we outline the development of zebrafish-optimized zdCas9-KRAB-MeCP2 and
111 zdCas9-VP64 CRISPR constructs. We establish their utility for efficient screening of candidate
112 gene function and disease relevance. Ongoing work in the lab will establish stable transgenic
113 lines expressing these proteins to facilitate rapid and systematic screening of gain and loss of
114 gene function by leveraging custom guide RNAs (gRNAs) to target promoters, 5'-UTR, or cell-
115 dependent cis-regulatory elements of selected candidate genes.

116 RESULTS
117

118 **CRISPRi modulates tyrosinase expression and its effect is observable between the prim**
119 **20-25 stages.**

120 To determine the functional capacity of zebrafish codon-optimized CRISPRi (Fig. 1A),
121 one-cell stage embryos of wild-type AB (WT AB) zebrafish were injected with CRISPRi mRNA
122 and target sgRNAs. As part of a series of proof-of-concept experiments, we designed sgRNAs
123 targeting the promoter region and 5'-UTR of the tyrosinase (*tyr*) gene, predicting that inhibition

124 would lead to diminished larval pigmentation, similar to established loss of function studies at this
125 locus (30,32,40).

126 Initially, sgRNAs were designed to target the *tyr* promoter or 5'-UTR (Methods) and one-
127 cell embryos (n ≥ 200) were injected with CRISPRi (100-300 ng/µl, final concentration) and a
128 cocktail of all five sgRNAs (150 ng/µl/each, final concentration). Zebrafish larvae assayed at the
129 prim 20-25 stages (33-36 hpf) displayed marked reduction in pigmentation of melanocytes (Fig.
130 1B), consistent with phenotypes arising from loss of function alleles in zebrafish (30) and other
131 vertebrates (39). By contrast, larvae receiving only the CRISPRi mRNA (n ≥ 200) or uninjected
132 (WT AB) controls (n ≥ 200), displayed no diminution in melanization at these stages. As expected,
133 the observed suppression of *tyr* dissipated over time, and by the pec-fin stage (60 hpf), reduction
134 in melanization was less noticeable in larvae receiving CRISPRi plus the cocktail of all sgRNAs
135 (Fig. 1B).

136 We measured the percentage of pigmentated area, imaged laterally, from a sample (n =
137 10) of larvae from each condition, at the prim 20-25 stage, and found a statistically significant
138 reduction of pigmentation between uninjected control (WT AB) and larvae injected with CRISPRi
139 plus all *tyr* sgRNAs (*p-value* = 1.263e-06, Fig. 1C, Supplemental Table 4a). We also observed a
140 statistically significant reduction of pigmentation between injected control (embryos injected with
141 CRISPRi mRNA only) and larvae injected with CRISPRi plus all *tyr* sgRNAs (*p-value* = 1.058e-
142 07, Fig. 1C, Supplemental Table 4a). We did not observe a statistically significant difference
143 between injected and uninjected controls (*p-value* = 0.5018, Fig. 1C, Supplemental Table 4a). We
144 subsequently performed the same pigmentation analysis at the pec-fin stage and observed the
145 same trend of hypopigmentation in CRISPRi plus all *tyr* sgRNAs (Fig. 1B-C, Supplemental Table
146 4b). However, the results were not statistically significant across conditions (*p-values* = 0.1226,
147 0.1418, and 0.7671, respectively, Fig. 1C, Supplemental Table 4b), confirming that the effects of
148 CRISPRi mRNA injection diminish over time.

149 We tested if delivery of each individual *tyr* sgRNAs could similarly silence transcription of
150 *tyr* and reduce melanin production. One of the five sgRNAs that we tested, sgRNA4 targeting the
151 promoter, efficiently modulated *tyr* expression (Supplemental Fig. 1), resulting in
152 hypopigmentation within prim 20-25 (33-36 hpf). We used this sgRNA to assess the optimal
153 concentration of CRISPRi and injected larvae each with 100 ng/µl, 300 ng/µl, and 500 ng/µl of
154 CRISPRi along with sgRNA4 (150 ng/µl). Our observations suggest no advantage to injecting
155 more than 300 ng/µl (final concentration) of CRISPRi mRNA (Supplemental Fig. 1). These results
156 demonstrate the effectiveness in modulating *tyr* by employing our zebrafish codon-optimized
157 CRISPRi with individual or pooled sgRNAs to target a gene's promoter. To build on these
158 observations, we sought to confirm the hypopigmentation phenotype by targeting other key
159 pigment genes that act upstream and are known to regulate *tyr*.
160

161 **CRISPRi targeting of *sox10* impedes epidermal pigmentation zebrafish**

162 Having established that *tyr* can be modulated via CRISPRi, we sought to evaluate a
163 broader applicability of our strategy, evaluating the effect of modulating genes upstream from *tyr*
164 in melanocyte differentiation, for which we predict overlapping phenotypic outcomes. We first
165 investigated whether *sox10*, the gene that encodes for a transcription factor known to be key to
166 promote melanin production in zebrafish and other vertebrates (35,36) could be silenced via
167 CRISPRi. We designed sgRNAs to target the promoter of the *sox10* gene, predicting that silencing
168 it would lead to downregulation of downstream pigment genes, *mitfa* and *tyr*, and subsequent
169 hypopigmentation in the zebrafish.

170 Four sgRNAs were designed to target the *sox10* promoter (Methods). Zebrafish larvae (n
171 ≥ 200) injected with CRISPRi (100-300 ng/µl, final concentration) plus a cocktail of all *sox10*
172 sgRNAs (150 ng/µl/each, final concentration) displayed marked reduction in pigmentation of
173 epidermal melanocytes, assayed at prim 20-25 (33-36 hpf), consistent with reduction of
174 pigmentation when targeting downstream gene *tyr* (Fig. 2A, Supplemental Fig. 2). Furthermore,

175 we observed that sgRNA3 was effective at reducing pigmentation when injected individually with
176 CRISPRi (Fig. 2A, Supplemental Fig. 2). We measured the percentage of pigmented area,
177 imaged laterally at the prim 20-25 stage, from a sample (n = 10) of larvae from each condition
178 and found a statistically significant reduction of pigmentation between uninjected control (WT AB)
179 and larvae injected with CRISPRi plus all *sox10* sgRNAs and CRISPRi plus *sox10* sgRNA3 (*p-*
180 *value* = 7.389e-07, 2.724e-06, respectively, Fig. 2B, Supplemental Table 5a). We also observed
181 a statistically significant reduction of pigmentation between injected control (embryos injected with
182 CRISPRi mRNA only) and larvae injected with CRISPRi plus all *sox10* sgRNAs and CRISPRi
183 plus *sox10* sgRNA3 (*p-value* = 8.704e-09, 3.243e-06, respectively, Fig. 2B, Supplemental Table
184 5a). Further, we did not observe a statistically significant reduction in pigmentation between larvae
185 receiving only the CRISPRi mRNA (n ≥ 200) and uninjected (WT AB) controls (n ≥ 200) (*p-value*
186 = 0.097, Fig. 2B, Supplemental Table 5a). The effects of CRISPRi dissipated by the pec-fin stage
187 (60 hpf) as the pigmentation patterns between injected and uninjected were indistinguishable (Fig.
188 2A, Supplemental Table 5b). When measuring the percentage of pigmented area at this stage,
189 we only observed at statistically significant reduction in pigmentation between WT AB and
190 CRISPRi plus all *sox10* sgRNAs (*p-value* = 0.019, Fig. 2B, Supplemental Table 5b). We did not
191 observe a statistically significant reduction in pigmentation across the other conditions (*p-value* =
192 0.481, 0.090, 0.999, 0.454, and 0.102, respectively, Fig. 2B, Supplemental Table 5b), which
193 confirms our observation that as larvae grow, the effects of CRISPRi mRNA injections dissipate.
194 It is noteworthy to mention that larvae injected with CRISPRi plus sgRNAs appear to be slightly
195 developmentally delayed as compared to controls, which may be the result of injection variability,
196 nucleic acid toxicity, or off-target effects. This is also consistent with an observed reduction in
197 retinal pigment epithelium (RPE) pigmentation within Prim 20-25 in larvae injected with CRISPRi
198 plus sgRNAs as well as in those injected with CRISPRi alone, as compared to WT (*p-value* =
199 0.048, Supplemental Fig. 2B, Supplemental Table 6). Given that these effects are not consistent
200 with the established loss of function phenotypes for these genes (33) , we do not score or interpret

201 RPE phenotypes throughout. However, the overall results are in line with previous work that
202 demonstrated that *sox10* is important for melanocyte development and melanin production with
203 its role in activating *tyr*, the rate-determining enzyme in melanin production (30,35,39,40). To
204 exclude the possibility of off-target effects by *sox10* sgRNA, we employed sgRNA3 and standard
205 CRISPR/Cas9 to establish correct targeting of the *sox10* promoter. Employing a standard T7
206 endonuclease I (T7EI) assay (Methods) we confirm that sgRNA3 is effective at guiding Cas9 to
207 the *sox10* promoter to induce double-strand breaks. We collected various clutches (n = 50) of WT
208 AB, CRISPR/Cas9 only, and CRISPR/Cas9 plus sgRNA3 and extracted genomic DNA to amplify
209 the *sox10* promoter. PCR amplification (Oligonucleotide primers: Forward: 5'-
210 CTCCCAACTCTTATTAACGA-3'; Reverse: 5'- ACACAGAGTAAGCGATAGAG-3') of this locus
211 and subsequent treatment with T7EI resulted in heteroduplex formation, indicating effective
212 targeting of *sox10* (Supplemental Fig. 2C).
213
214 **Effective CRISPRi modulation of *mitfa* limits epidermal melanin production.**
215 Extending from our results modulating *sox10* and *tyr* expression, we next evaluated
216 whether targeting the gene encoding the transcription factor mitfa would also induce
217 hypopigmentation. The *mitfa* gene plays critical roles in pigmentation throughout vertebrates
218 (*MITF/Mitf*), activating *tyr* transcription during early development (35,59). We designed sgRNAs
219 to target the promoter and 5'-UTR regions of the *mitfa* gene, predicting that, as with known loss-
220 of-function (LoF) alleles (34,59), titrating activity of this transcription factor would also result in
221 reduced activation of *tyr* in epidermal melanocytes and thus lower melanization across the body.
222 Four sgRNAs were designed to target the *mitfa* promoter (Methods). As before, zebrafish
223 one-cell embryos (n ≥ 200) injected with CRISPRi (100-300 ng/µl, final concentration) and a
224 cocktail of all *mitfa* sgRNAs (150 ng/µl/each, final concentration) displayed marked reduction in
225 pigmentation of epidermal melanocytes, assayed at prim 20-25 (33-36 hpf) (Fig. 2C). This is
226 consistent with prior *mitfa* LoF studies (60) where failure to express *mitfa* prevents the production

227 of melanocyte precursors, leading to reduced global pigmentation in zebrafish larvae. In contrast,
228 no reduction in pigmentation was observed in larvae receiving only the CRISPRi mRNA (n ≥ 200)
229 or uninjected (WT AB) controls (n ≥ 200) (Fig. 2C). Additionally, a single *mitfa* sgRNA targeting
230 the promoter or 5'-UTR effectively silenced *mitfa,* resulting in marked reduction of melanin
231 production at prim 20-25 (33-36 hpf) (Supplemental Fig. 3). Silencing of *mitfa* dissipated over time
232 and by the pec-fin stage (60 hpf), melanization was similar between controls and injected larvae
233 (Fig. 2C, Supplemental Fig. 3). These results are consistent with the hypopigmentation phenotype
234 in epidermal melanocytes that is observed when modulating the *tyr* gene (Fig. 1B-C) and
235 transcription of *sox10* (Fig. 2A-B).
236
237 **CRISPRi/a affects zebrafish length by modulating transcription of *mrap2a***
238 To build upon the successful demonstration of CRISPRi-mediated modulation of zebrafish
239 pigmentation, we set out to test our CRISPRa (Fig. 1A) system focusing on somatic size (length).
240 The benefit of this phenotype is that it provides the opportunity for evaluation of both reduction
241 and increase in gene function. We targeted the *mrap2a* gene which is known to regulate the
242 expression of the melanocortin 4 receptor (*mc4r*) gene by downregulating its transcription (50,62).
243 Both genes have been shown to be involved in energy homeostasis and somatic growth in mice
244 and zebrafish; and are thought to be involved in a significant portion of familial early-onset obesity
245 in humans (63). We predicted that targeting *mrap2a* with CRISPRa and further increasing its
246 transcription would result in a decrease in *mc4r* transcription, which would lead to an increase in
247 larval length. By contrast, downregulating *mrap2a* with CRISPRi would lead to an increase in
248 *mc4r* expression, resulting in larvae shorter in length (50,63).
249 While a range of loss-of-function experiments have been performed targeting *mrap2a*
250 (50,62,63), gain-of-function (GoF) experiments targeting *mrap2a* have not been explored. We
251 designed four sgRNAs to target the *mrap2a* promoter (Methods) with our CRISPRa system.
252 Zebrafish larvae (n ≥ 200) injected with CRISPRa (100-300 ng/µl, final concentration) and a

253 cocktail of all *mrap2a* sgRNAs (150 ng/µl/each, final concentration) displayed marked increase in
254 body length, assayed at the pec-fin stage (60 hpf) (Fig. 3A). Similarly, we tested if an individual
255 sgRNA could guide the dCas9-VP64 to modulate body length and found sgRNA3 capable of
256 inducing an observable phenotype (Fig. 3A-B). By contrast, no increase in larval length was
257 observed at the pec-fin stage (60 hpf) in larvae receiving only the CRISPRa mRNA (n ≥ 200) or
258 in uninjected (WT AB) controls (n ≥ 200). Moreover, the effects of CRISPRa were still noticeable
259 at the day 5 stage (120 hpf) and at the day 7 stage (168 hpf), as the length of these larvae was
260 still longer than control conditions (Fig. 3A, Supplemental Fig. 4). Furthermore, we measured the
261 length of larvae receiving CRISPRa plus sgRNA3 (n = 50), sgRNA3-only (n = 50), and uninjected
262 (WT AB) controls (n = 50) and performed a Welch two-sample t-test to analyze if the average
263 length between these conditions was statistically different (Fig. 3B, Supplemental Table 7). At the
264 pec-fin stage (60 hpf), the average length for these conditions was 3673.67 µm, 3468.86 µm, and
265 3466.28 µm (*p-value* = 8.58e-16; 1.83e-14, and 0.9181), respectively. The longer larval length
266 phenotype due to increased *mrap2a* transcription and decreased *mc4r* expression is consistent
267 with increased size and weight in mice that become obese due to *mc4r* haploinsufficiency (29),
268 and with morbid obesity cases in humans due to frameshift (loss of function) mutations in *mc4r*
269 (64).

270 We used the same sgRNAs to target and impede *mrap2a* and increase *mc4r* expression.
271 Zebrafish larvae (n ≥ 200) injected with CRISPRi (100-300 ng/µl, final concentration) plus all
272 sgRNAs (150 ng/µl/each, final concentration) displayed a decrease in larval length at the pec-fin
273 stage (60 hpf) (Fig. 3A, 3C), which is consistent with rescuing obese mice with *mc4r*
274 haploinsufficiency (29). Additionally, sgRNA3 was able to guide the CRISPRi to modulate
275 silencing of *mrap2a* individually and led to a decrease in larval length, observed at the pec-fin
276 stage (60 hpf) (Fig. 3A. 3C). By contrast, larval length observed at the pec-fin stage (60 hpf) for
277 larvae receiving only the CRISPRi mRNA (n ≥ 200) or in uninjected (WT AB) controls (n ≥ 200)
278 was higher than our experimental condition (Fig. 3A). Further, larvae injected with CRISPRi still

279 displayed a shorter length around the day 5 stage (120 hpf); however, their length was similar to
280 controls at the day 7 stage (168 hpf) (Fig. 3A, Supp Fig. 4). We also measured the larval length
281 for the conditions CRISPRi plus sgRNA3 (n = 50), sgRNA3-only (n = 50), and uninjected (WT AB)
282 controls (n = 50) at the pec-fin stage (60 hpf) and found their average length to be 3481.98 μm,
283 3779.96 μm, and 3748.82 μm, respectively (Fig. 3B, Supplemental Table 8). We analyzed the
284 statistical significance between these means with a Welch two-sample t-test and found the
285 difference in means between experimental and control conditions to be statistically significant (*p-*
286 *value* = 2.2e-16, 2.2e-16, and 0.0636). Although highly significant, the observed magnitude of
287 effect may potentially be further enhanced by simultaneous modulation of the agouti-related
288 protein (agrp), which Sebag et al. demonstrated acted in concert with *mrap2a* in antagonism of
289 *mc4r* (50).

290 DISCUSSION
291

292 CRISPRi/a has emerged as a powerful tool in genetic research, offering the ability to
293 modulate gene expression both for exploration of fundamental mechanisms and for potential
294 therapeutics. It offers the capacity to modulate gene expression without inducing genetic
295 alterations which makes CRISPRi/a valuable technology for the study of gene regulation and for
296 efficient exploration of both gain and loss of function phenotypes. Nevertheless, their development
297 and application in zebrafish have been slow over the past decade, with only one study describing
298 an effort to implement it (26), while many others apply CRISPR-based editing technologies
299 (18,19,21,53,54,65).

300 In this study, we chose to fuse a catalytically inactive Cas9 with the transcriptional
301 repressor KRAB-MeCP2. Our choice to use dCas9-KRAB-MeCP2 was guided by previous
302 studies that demonstrated its ability to induce gene silencing while outperforming dCas9-KRAB
303 systems (24,66) implemented in previous CRISPRi experiments in zebrafish (26). In contrast, for

304 our CRISPRa system, we fused the dCas9 with the transcriptional activator VP64. Comparisons
305 between different Cas9 activators have demonstrated the VP64 to effectively induce gene
306 activation (25). While other Cas9 activators such as VPR, SAM, and Suntag have been shown to
307 outperform VP64, these systems have not been tested in zebrafish and/or require special sgRNAs
308 to induce their effect. By using a catalytically inactive Cas9 fused with the transcriptional
309 repressors KRAB-MeCP2 or the transcriptional activator VP64, we have achieved transcriptional
310 control over key genes involved in melanocyte differentiation (*sox10* and *mitfa*), pigmentation (*tyr*),
311 and somatic growth (*mrap2a*) in zebrafish. Our results underscore the versatility and efficiency of
312 CRISPRi/a in zebrafish research. For instance, by independently downregulating *sox10, mitfa,*
313 and *tyr*, we established zebrafish larvae with marked reduction in pigmentation. Similarly, by
314 activating or downregulating *mrap2a*, we successfully modulated larval length.

315 These proof-of-principle experiments underscore the potential of CRISPRi/a technology
316 to control gene expression by targeting gene promoters. CRISPRi/a is relatively straightforward
317 to implement compared to other genetic editing technologies, which further increases its appeal.
318 In addition, implementing this technology in transparent one-cell zebrafish embryos makes it
319 easier to study the effects of gene silencing and activation during development. Further,
320 CRISPRi/a can be implemented to study the effects of silencing or activating noncoding regulatory
321 sequences such as enhancers, repressors, and insulators. Taking advantage of the fact that
322 approximately 70% of human genes have a zebrafish gene homolog facilitates the study of gene
323 regulatory mechanisms and networks in yet another vertebrate system. The versatility to study
324 gene expression modulation, by either targeting gene promoters or any potential noncoding
325 regulatory sequences in a vertebrate system, can offer insights into disease pathogenesis and
326 therapeutic targets that may translate to clinical applications. Further, our evaluation of *mrap2a*
327 modulation also demonstrates that modulating the regulation of one gene can elicit indirect
328 regulation of other target genes, opening the door to a better understanding of gene regulatory
329 networks and their exploration for potential therapeutic interventions.

330 CRISPRi/a technologies, just like CRISPR gene editing, can also be limited by off-target
331 effects and variability in efficiency across genomic loci. Additionally, the ethical implications of
332 gene expression modulation and the potential for unintended consequences underscore the
333 importance of careful consideration in the application of this technology. In this current study, the
334 primary limitation is the delivery of CRISPRi/a via mRNA microinjections, which is titrated as the
335 embryo develops and the larvae grow older. Furthermore, developmental delays can occur in
336 larvae injected with foreign mRNA, which further reflects the variability induced by the combination
337 of mRNA microinjections, potential off-target effects, and nucleic acid toxicity. This results in a
338 diminution of molecular and observable phenotypes and hinders the potential to study long-term
339 effects of gene expression modulation, making it difficult to elucidate any potential disease
340 relevance. To this end, we are actively generating stable transgenic lines expressing CRISPRi/a
341 to facilitate rapid and systematic screening of gain or loss of gene function. Our ongoing work will
342 expand the zebrafish toolkit, establishing the utility of CRISPRi/a for evaluation of candidate gene
343 function and disease relevance.

344 METHODS
345

346 **Generation of catalytically inactive Cas9 plasmid vector**

347 The zebrafish optimized *Cas9* gene within the plasmid vector pT3TS-nCas9n (Addgene
348 #46757) was mutated to produce a catalytically inactive dead *Cas9* (dCas9). The DNA sequence
349 corresponding to the RuvC-like and HNH nuclease domains of the Cas9 protein were modified
350 by inducing a change from Aspartic acid to Alanine at position 10 (D10A), and a change from
351 Histidine to Alanine at position 839 (H839A). This was accomplished by implementing the
352 NEBuilder HiFi DNA Assembly (Cat. # E5520S) protocol using oligonucleotides primers
353 (Supplemental Table 1) generated using the NEBuilder Assembly Tool (v.2.10.1). The modified
354 plasmid vector was then transformed into NEB 5-a competent *E. coli* cells (Cat. # C2987I) and

355 later mini-prepped using NEB Monarch Plasmid Miniprep Kit (Cat. # T1010L). The plasmid vector
356 generated was named pT3TS-ndCas9n.
357
358 **Codon Optimization of KRAB-MeCP2 and VP64 domains for zebrafish usage**
359 The DNA sequence for the KRAB-MeCP2 repressor was obtained from the dCas9-KRAB-
360 MeCP2 plasmid vector (Addgene #110821); while the DNA sequence for the VP64 activator was
361 obtained from the dCas9-VP64-GFP plasmid vector (Addgene #61422). The codon optimization
362 tool from IDT was used to optimize these sequences for zebrafish. The KRAB-MeCP2 repressor
363 sequence (1,263 bp) containing an SV40 NLS before and after KRAB was optimized and ordered
364 as a gBlocks HiFi Gene Fragment. The VP64 activator sequence (225 bp) containing an SV40
365 NLS before VP64 was optimized and ordered as a gBlocks Gene Fragment.
366
367 **CRISPRi/a plasmid construct generation and *in vitro* transcription**
368 The codon optimized KRAB-MeCP2 repressor and VP64 activator were cloned into the
369 pT3TS-ndCas9n plasmid vector containing a catalytically inactive dCas9 sequence. Cloning was
370 carried out by employing NEBuilder HiFi DNA Assembly (Cat. # E5520S) using oligonucleotide
371 primers (Supplemental Table 2) that overlapped both the target region of the plasmid vector and
372 the optimized sequences. Once the optimized sequences had been cloned in, the plasmid
373 constructs were transformed into NEB 5-a competent *E. coli* cells (Cat. # C2987I) and later mini-
374 prepped using NEB Monarch Plasmid Miniprep Kit (Cat. # T1010L). The plasmid constructs
375 generated were named zdCas9-KRAB-MeCP2 and zdCas9-VP64 for CRISPRi and CRISPRa,
376 respectively.
377 The restriction enzyme XbaI (NEB Cat # R0145) was used to linearize the CRISPRi/a
378 plasmid constructs. Subsequently, *in vitro* transcription of the d*Cas9* gene plus the repressor or
379 activator was performed by employing the mMessage mMachine T3 Transcription kit (Cat. #

380 AM1348). RNA was recovered by using the RNA Clean-up protocol from the Qiagen RNeasy Mini
381 Kit (Cat. # 74104) and stored at -80°C.
382
383 **Designing targeted gRNAs for CRISPRi/a**
384 Multiple single guide RNAs (sgRNAs) were designed to target the promoter or 5'-UTR of
385 the various genes in the zebrafish. All sgRNAs followed a core 5'-N18-3'(53) sequence and were
386 designed using the online tool CRISPOR (PMID: 29762716). At the 5' end of the forward
387 oligonucleotide, the nucleotides 5'-TAGG-3' were added. At the 5' end of the reverse
388 oligonucleotide (reverse complement of N18 sequence), the nucleotides 5'-AAAC-3' were added.
389 The final form of the oligonucleotides was 5'-TAGG-N18-3' for the forward oligo; and 5'-AAAC-
390 N18RevCompl-3'. The oligo primers for each sgRNA were ordered from IDT (Supplemental Table
391 3). Oligonucleotide primers were first annealed and subsequently cloned into the pT7-gRNA
392 plasmid vector (Addgene #46759) containing a gRNA scaffold, according to restriction enzyme
393 cloning protocol specifications from previous studies(54). After cloning, each plasmid construct
394 generated for each sgRNA was transformed into NEB 5-a competent *E. coli* cells (Cat. # C2987I)
395 and later mini-prepped using NEB Monarch Plasmid Miniprep Kit (Cat. # T1010L). Linearization
396 of these constructs was performed using the restriction enzyme BamHI-HF (NEB Cat # R3136).
397 The linear DNA was purified using the Zymo Research DNA Clean & Concentrator-5 protocol
398 (Cat. # D4013). Subsequently, *in vitro* transcription of linear DNA was performed using the
399 Thermo Fisher MEGAshortscript T7 Kit (Cat. # AM1354) or the NEB HiScribe T7 High Yield RNA
400 Synthesis Kit (Cat. #E2040S). After in vitro transcription, RNA was recovered by using the RNA
401 Clean-up protocol from the Qiagen RNeasy Mini Kit (Cat. # 74104) and stored at -80°C.
402
403 **Zebrafish husbandry and microinjections of one-cell stage embryos**
404 We used the zebrafish AB strain (ZFIN ID: ZDB-GENO-960809-7) as our wild-type fish
405 (WT AB). The day before injections, adult AB zebrafish crosses were set up in tanks with dividers

406 at a ratio of 2:1 or 3:2 females per male. The morning of injections and when the lights came on,
407 the dividers were removed to allow for mating among zebrafish. Zebrafish embryos were injected
408 during the first 15-20 mins after being collected to ensure injection occurred at the one-cell stage.
409 The mixture injected to the embryos contain CRISPRi/a mRNA (100-300 ng/µl, final
410 concentration), sgRNA mRNA (150 ng/µl/each, final concentration), 0.2 µl of Phenol Red, and
411 Nuclease Free Water up to 5 µl. After microinjections, zebrafish embryos were incubated at 28°C
412 in E3 embryo medium provided by Johns Hopkins FinZ Zebrafish Core Center.
413

414 **Zebrafish length measurement and image collection**

415 All zebrafish larvae used for measurements or image collection were staged according to
416 anatomical hallmarks described in Kimmel *et al*(55). Larvae were anesthetized using ethyl-3-
417 aminobenzoate methanesulfonate salt (Tricane/MS-222; Sigma Aldrich #E10521) prepared at a
418 concentration of 4 mg/mL using 1 M Tris (pH 9, 4% v/v). The Nikon AZ100 Multizoom fluorescent
419 microscope was used for both measurements and image collection at a ratio of 3.22 µm/px. For
420 all images, zebrafish larvae were suspended in 3% Methyl Cellulose (Sigma Aldrich #M0387)
421 solution. Larvae were imaged and measured at pec-fin, day 5, and day 7 stages and p-values
422 were calculated using the Welch two-sample t-test.
423

424 **Pigment quantification analysis in ImageJ**

425 To assess variation of pigmentation across conditions, we used ImageJ(56) to measure
426 the total area of pigmentation in larvae within the prim 20-25 stages and at the pec-fin stages,
427 across treatment conditions. For this, lateral and dorsal view images were used to assess the
428 level of pigmentation in epidermal melanocytes and in the RPE, respectively. Briefly, we employed
429 a previously published pipeline(57) with minor modifications in the selection of the region of
430 interest (ROI). We first converted all images to 16-bit images before selecting the ROI. We then
431 created a mask from the ROI and followed by using the threshold function with default

432 thresholding method. Next, we restored the selection and used the analyze particle function to
433 measure the area of pigmentation within the ROI. For analyzing lateral view images, the contour
434 of the larvae, without eyes and the yolk sac, was selected as the ROI. The eyes were excluded
435 due to the superimposition of one eye over the other from a lateral view increasing the total
436 pigmentation in one eye. The yolk sac, but not the yolk sac extension, was also excluded from
437 lateral view analysis due to the level of shade in the periphery of the sac. The dorsal view images
438 were utilized to analyze the total area of pigmentation in the eyes. Larvae were imaged and
439 measured at prim 20-25 and pec-fin stages and p-values were calculated using the Welch two-
440 sample t-test.
441
442 **T7 Endonuclease I (T7EI) assay for heteroduplex detection**
443 Zebrafish embryos (n > 250) were injected with zebrafish-optimized *Cas9* mRNA (300
444 ng/µl, final concentration) that was *in-vitro* transcribed from the linearized pT3TS-nCas9n
445 (Addgene #46757) plasmid vector. The microinjection mixture also included synthesized sgRNA
446 mRNA (150 ng/µl, final concentration), nuclease-free water, and phenol red. At 48 hours post
447 injection, clutches of 50 embryos per condition were collected for DNA extraction. DNA extraction
448 was performed by incubating embryo clutches in 50 µl of zebrafish lysis buffer (1M Tris pH 8.4,
449 1M KCl, 1M $MgCl_2$, 20% Tween-20, and 10% NP-40) at 94°C for 20 mins, 55°C (Hold to add 10
450 mg/ml Proteinase K), 55°C for 60 mins, 94°C for 20 mins, and optionally incubating at 4°C.
451 Following extraction, DNA was amplified following standard PCR amplification protocols and
452 purified using the Zymo Research DNA Clean & Concentrator-5 protocol (Cat. # D4013). The
453 standard protocol from the T7EI assay from NEB (Cat. #M0689) was followed and after digestion,
454 results were visualized in a 2% agarose gel.
455
456 **Ethics Statement**

457 All zebrafish maintenance, handling, and analyses were performed under approved
458 protocols from the Johns Hopkins University Animal Care and Use Committee (Protocol #
459 FI22M203)
460
461 AUTHOR CONTRIBUTIONS: A.S.M., V.C.C, and N.B.B. conceptualized the study. N.B.B.
462 designed codon optimized dCas9-KRAB-MeCP2 and dCas9-VP64 constructs and custom single
463 guide RNAs. N.B.B., E.A.S., and R.J.B. injected RNA constructs into zebrafish embryos. N.B.B.
464 and E.A.S. imaged the fish. N.B.B. and R.J.B. wrote the manuscript. All authors edited and
465 approved the final manuscript for publication.
466
467 FUNDING: This research, undertaken at Johns Hopkins University School of Medicine, was
468 supported in part by awards from the National Institutes of Health to A.S.M. (R21HD120879),
469 V.C.C. (R35GM136644), as well as N.B.B., E.A.S., and R.J.B. (T32GM148383-01); and by the
470 Canadian Institutes of Health Research (DFD-181599) to R.J.B.
471
472 ACKNOWLEDGEMENTS: The authors would like to acknowledge the FInZ Zebrafish Core
473 Center for assistance with zebrafish husbandry.
474
475 CONFLICTS OF INTEREST: The authors declare no competing interests.
476

477 REFERENCES

478

479 1. Giffen KP, Liu H, Kramer KL, He DZ. Expression of Protein-Coding Gene Orthologs in
480 Zebrafish and Mouse Inner Ear Non-sensory Supporting Cells. Front Neurosci [Internet].
481 2019 Oct 18 [cited 2024 Aug 28];13. Available from: /pmc/articles/PMC6813431/

482 2. Howe K, Clark MD, Torroja CF, Torrance J, Berthelot C, Muffato M, et al. The zebrafish
483 reference genome sequence and its relationship to the human genome. Nature [Internet].
484 2013 Apr 25 [cited 2024 Aug 28];496(7446):498–503. Available from:
485 https://pubmed.ncbi.nlm.nih.gov/23594743/

486 3. Fisher S, Grice EA, Vinton RM, Bessling SL, Urasaki A, Kawakami K, et al. Evaluating
487 the biological relevance of putative enhancers using Tol2 transposon-mediated
488 transgenesis in zebrafish. Nature Protocols 2006 1:3 [Internet]. 2006 Oct 12 [cited 2022
489 Feb 15];1(3):1297–305. Available from: https://www.nature.com/articles/nprot.2006.230

490 4. Gorkin DU, Lee D, Reed X, Fletez-Brant C, Bessling SL, Loftus SK, et al. Integration of
491 ChIP-seq and machine learning reveals enhancers and a predictive regulatory sequence
492 vocabulary in melanocytes. Genome Res [Internet]. 2012 Nov [cited 2024 Aug
493 28];22(11):2290–301. Available from: https://pubmed.ncbi.nlm.nih.gov/23019145/

494 5. Fisher S, Grice EA, Vinton RM, Bessling SL, McCallion AS. Conservation of RET
495 regulatory function from human to zebrafish without sequence similarity. Science
496 [Internet]. 2006 Apr 14 [cited 2024 Aug 28];312(5771):276–9. Available from:
497 https://pubmed.ncbi.nlm.nih.gov/16556802/

498 6. Antonellis A, Huynh JL, Lee-Lin SQ, Vinton RM, Renaud G, Loftus SK, et al. Identification
499 of neural crest and glial enhancers at the mouse Sox10 locus through transgenesis in
500 zebrafish. PLoS Genet [Internet]. 2008 Sep [cited 2024 Aug 28];4(9). Available from:
501 https://pubmed.ncbi.nlm.nih.gov/18773071/

502 7. Doyle AJ, Doyle JJ, Bessling SL, Maragh S, Lindsay ME, Schepers D, et al. Mutations in
503 the TGF-β repressor SKI cause Shprintzen-Goldberg syndrome with aortic aneurysm.
504 Nat Genet [Internet]. 2012 Nov [cited 2024 Aug 28];44(11):1249–54. Available from:
505 https://pubmed.ncbi.nlm.nih.gov/23023332/

506 8. Gould RA, Aziz H, Woods CE, Seman-Senderos MA, Sparks E, Preuss C, et al. ROBO4
507 variants predispose individuals to bicuspid aortic valve and thoracic aortic aneurysm. Nat
508 Genet [Internet]. 2019 Jan 1 [cited 2024 Aug 28];51(1):42–50. Available from:
509 https://pubmed.ncbi.nlm.nih.gov/30455415/

510 9. Golzio C, Willer J, Talkowski ME, Oh EC, Taniguchi Y, Jacquemont S, et al. KCTD13 is a
511 major driver of mirrored neuroanatomical phenotypes of the 16p11.2 copy number
512 variant. Nature [Internet]. 2012 May 17 [cited 2024 Aug 28];485(7398):363–7. Available
513 from: https://pubmed.ncbi.nlm.nih.gov/22596160/

514 10. Panizzi JR, Becker-Heck A, Castleman VH, Al-Mutairi DA, Liu Y, Loges NT, et al.
515 CCDC103 mutations cause primary ciliary dyskinesia by disrupting assembly of ciliary
516 dynein arms. Nat Genet [Internet]. 2012 Jun [cited 2024 Aug 28];44(6):714–9. Available
517 from: https://pubmed.ncbi.nlm.nih.gov/22581229/

11. Roscioli T, Kamsteeg EJ, Buysse K, Maystadt I, Van Reeuwijk J, Van Den Elzen C, et al. Mutations in ISPD cause Walker-Warburg syndrome and defective glycosylation of α-dystroglycan. Nat Genet [Internet]. 2012 May [cited 2024 Aug 28];44(5):581–5. Available from: https://pubmed.ncbi.nlm.nih.gov/22522421/

12. Tobin DM, Roca FJ, Oh SF, McFarland R, Vickery TW, Ray JP, et al. Host genotype-specific therapies can optimize the inflammatory response to mycobacterial infections. Cell [Internet]. 2012 Feb 3 [cited 2024 Aug 28];148(3):434–46. Available from: https://pubmed.ncbi.nlm.nih.gov/22304914/

13. Maragh S, Miller RA, Bessling SL, McGaughey DM, Wessels MW, De Graaf B, et al. Identification of RNA binding motif proteins essential for cardiovascular development. BMC Dev Biol [Internet]. 2011 [cited 2024 Aug 28];11. Available from: https://pubmed.ncbi.nlm.nih.gov/22011202/

14. Wahbeh MH, Boyd RJ, Yovo C, Rike B, McCallion AS, Avramopoulos D. A functional schizophrenia-associated genetic variant near the TSNARE1 and ADGRB1 genes. HGG Adv [Internet]. 2024 Jul 18 [cited 2024 Aug 28];5(3). Available from: https://pubmed.ncbi.nlm.nih.gov/38702885/

15. Asakawa K, Kawakami K. Targeted gene expression by the Gal4-UAS system in zebrafish. Dev Growth Differ [Internet]. 2008 Aug 1 [cited 2024 Sep 8];50(6):391–9. Available from: https://onlinelibrary.wiley.com/doi/full/10.1111/j.1440-169X.2008.01044.x

16. Zhu C, Smith T, Mcnulty J, Rayla AL, Lakshmanan A, Siekmann AF, et al. Evaluation and application of modularly assembled zinc-finger nucleases in zebrafish. Development [Internet]. 2011 Oct 15 [cited 2024 Sep 8];138(20):4555–64. Available from: http://www.r-project.org

17. Huang P, Xiao A, Zhou M, Zhu Z, Lin S, Zhang B. Heritable gene targeting in zebrafish using customized TALENs. Nature Biotechnology 2011 29:8 [Internet]. 2011 Aug 1 [cited 2024 Sep 8];29(8):699–700. Available from: https://www.nature.com/articles/nbt.1939

18. Hwang WY, Fu Y, Reyon D, Maeder ML, Tsai SQ, Sander JD, et al. Efficient genome editing in zebrafish using a CRISPR-Cas system. Nat Biotechnol [Internet]. 2013 Mar [cited 2024 Aug 28];31(3):227–9. Available from: https://pubmed.ncbi.nlm.nih.gov/23360964/

19. Shah AN, Davey CF, Whitebirch AC, Miller AC, Moens CB. Rapid reverse genetic screening using CRISPR in zebrafish. Nat Methods [Internet]. 2015 May 28 [cited 2024 Aug 28];12(6):535–40. Available from: https://pubmed.ncbi.nlm.nih.gov/25867848/

20. Varshney GK, Pei W, Lafave MC, Idol J, Xu L, Gallardo V, et al. High-throughput gene targeting and phenotyping in zebrafish using CRISPR/Cas9. Genome Res [Internet]. 2015 Jul 1 [cited 2024 Aug 28];25(7):1030–42. Available from: https://pubmed.ncbi.nlm.nih.gov/26048245/

21. Zhang Y, Qin W, Lu X, Xu J, Huang H, Bai H, et al. Programmable base editing of zebrafish genome using a modified CRISPR-Cas9 system. Nat Commun [Internet]. 2017 Dec 1 [cited 2024 Aug 28];8(1). Available from: https://pubmed.ncbi.nlm.nih.gov/28740134/

22. Hisano Y, Sakuma T, Nakade S, Ohga R, Ota S, Okamoto H, et al. Precise in-frame integration of exogenous DNA mediated by CRISPR/Cas9 system in zebrafish. Sci Rep [Internet]. 2015 [cited 2024 Aug 28];5. Available from: https://pubmed.ncbi.nlm.nih.gov/25740433/

23. Larson MH, Gilbert LA, Wang X, Lim WA, Weissman JS, Qi LS. CRISPR interference (CRISPRi) for sequence-specific control of gene expression. Nature Protocols 2013 8:11 [Internet]. 2013 Oct 17 [cited 2023 Jul 25];8(11):2180–96. Available from: https://www.nature.com/articles/nprot.2013.132

24. Yeo NC, Chavez A, Lance-Byrne A, Chan Y, Menn D, Milanova D, et al. An enhanced CRISPR repressor for targeted mammalian gene regulation. Nat Methods [Internet]. 2018 Aug 1 [cited 2023 Dec 19];15(8):611–6. Available from: https://pubmed.ncbi.nlm.nih.gov/30013045/

25. Chavez A, Tuttle M, Pruitt BW, Ewen-Campen B, Chari R, Ter-Ovanesyan D, et al. Comparison of Cas9 activators in multiple species. Nat Methods [Internet]. 2016 Jun 29 [cited 2024 Aug 28];13(7):563–7. Available from: https://pubmed.ncbi.nlm.nih.gov/27214048/

26. Long L, Guo H, Yao D, Xiong K, Li Y, Liu P, et al. Regulation of transcriptionally active genes via the catalytically inactive Cas9 in C. elegans and D. rerio. Cell Research 2015 25:5 [Internet]. 2015 Mar 27 [cited 2023 Aug 22];25(5):638–41. Available from: https://www.nature.com/articles/cr201535

27. Sastre D, Zafar F, Torres CAM, Piper D, Kirik D, Sanders LH, et al. Inactive S. aureus Cas9 downregulates alpha-synuclein and reduces mtDNA damage and oxidative stress levels in human stem cell model of Parkinson's disease. Sci Rep [Internet]. 2023 Dec 1 [cited 2024 Aug 28];13(1). Available from: https://pubmed.ncbi.nlm.nih.gov/37853101/

28. Matharu N, Ahituv N. Modulating gene regulation to treat genetic disorders. Nature Reviews Drug Discovery 2020 19:11 [Internet]. 2020 Oct 5 [cited 2023 Jul 25];19(11):757–75. Available from: https://www.nature.com/articles/s41573-020-0083-7

29. Matharu N, Rattanasopha S, Tamura S, Maliskova L, Wang Y, Bernard A, et al. CRISPR-mediated activation of a promoter or enhancer rescues obesity caused by haploinsufficiency. Science (1979) [Internet]. 2019 Jan 18 [cited 2023 Jul 24];363(6424). Available from: https://www.science.org/doi/10.1126/science.aau0629

30. Camp E, Lardelli M. Tyrosinase gene expression in zebrafish embryos. Dev Genes Evol [Internet]. 2001 [cited 2023 Aug 29];211(3):150–3. Available from: https://link.springer.com/article/10.1007/s004270000125

31. Cooper CD, Raible DW. Mechanisms for reaching the differentiated state: Insights from neural crest-derived melanocytes. Semin Cell Dev Biol [Internet]. 2009 [cited 2024 Aug 28];20(1):105–10. Available from: https://pubmed.ncbi.nlm.nih.gov/18935965/

32. Haffter P, Odenthal J, Mullins MC, Lin S, Farrell MJ, Vogelsang E, et al. Mutations affecting pigmentation and shape of the adult zebrafish. Dev Genes Evol [Internet]. 1996 [cited 2023 Aug 30];206(4):260–76. Available from: https://link.springer.com/article/10.1007/s004270050051

600 33. Lane BM, Lister JA. Otx but Not Mitf Transcription Factors Are Required for Zebrafish
601 Retinal Pigment Epithelium Development. PLoS One [Internet]. 2012 Nov 5 [cited 2024
602 Feb 18];7(11):49357. Available from: /pmc/articles/PMC3489725/

603 34. Lister JA, Close J, Raible DW. Duplicate mitf genes in zebrafish: complementary
604 expression and conservation of melanogenic potential. Dev Biol [Internet]. 2001 Sep 15
605 [cited 2023 Nov 28];237(2):333–44. Available from:
606 https://pubmed.ncbi.nlm.nih.gov/11543618/

607 35. Murisier F, Guichard S, Beermann F. The tyrosinase enhancer is activated by Sox10 and
608 Mitf in mouse melanocytes. Pigment Cell Res [Internet]. 2007 Jun 1 [cited 2023 Aug
609 29];20(3):173–84. Available from: https://onlinelibrary.wiley.com/doi/full/10.1111/j.1600-
610 0749.2007.00368.x

611 36. Dutton KA, Pauliny A, Lopes SS, Elworthy S, Carney TJ, Rauch J, et al. Zebrafish
612 colourless encodes sox10 and specifies non-ectomesenchymal neural crest fates.
613 Development [Internet]. 2001 Nov 1 [cited 2024 Aug 11];128(21):4113–25. Available
614 from: https://dx.doi.org/10.1242/dev.128.21.4113

615 37. Johnson SL, Nguyen ATN, Lister JA. mitfa is required at multiple stages of melanocyte
616 differentiation but not to establish the melanocyte stem cell. Dev Biol [Internet]. 2011 Feb
617 2 [cited 2024 Aug 28];350(2):405. Available from: /pmc/articles/PMC3040983/

618 38. Wang C, Kocher TD, Wu J, Li P, Liang G, Lu B, et al. Knockout of microphthalmia-
619 associated transcription factor (mitf) confers a red and yellow tilapia with few pigmented
620 melanophores. Aquaculture. 2023 Feb 25;565:739151.

621 39. Wu YC, Wang IJ. Heat-shock-induced tyrosinase gene ablation with CRISPR in
622 zebrafish. Molecular Genetics and Genomics [Internet]. 2020 Jul 1 [cited 2023 Aug
623 29];295(4):911–22. Available from: https://link.springer.com/article/10.1007/s00438-020-
624 01681-x

625 40. Camp E, Badhwar P, Mann GJ, Lardelli M. Expression Analysis of a Tyrosinase Promoter
626 Sequence in Zebrafish. Pigment Cell Res [Internet]. 2003 Apr 1 [cited 2023 Sep
627 10];16(2):117–26. Available from: https://onlinelibrary.wiley.com/doi/full/10.1034/j.1600-
628 0749.2003.00002.x

629 41. Frantz WT, Ceol CJ. From Tank to Treatment: Modeling Melanoma in Zebrafish. Cells
630 [Internet]. 2020 May 22 [cited 2024 Aug 28];9(5). Available from:
631 https://pubmed.ncbi.nlm.nih.gov/32455885/

632 42. Praetorius C, Grill C, Stacey SN, Metcalf AM, Gorkin DU, Robinson KC, et al. A
633 polymorphism in IRF4 affects human pigmentation through a tyrosinase-dependent
634 MITF/TFAP2A pathway. Cell [Internet]. 2013 Nov 21 [cited 2024 Aug 28];155(5):1022.
635 Available from: https://pubmed.ncbi.nlm.nih.gov/24267888/

636 43. Rosenbaum SR, Tiago M, Caksa S, Capparelli C, Purwin TJ, Kumar G, et al. SOX10
637 requirement for melanoma tumor growth is due, in part, to immune-mediated effects. Cell
638 Rep [Internet]. 2021 Dec 7 [cited 2024 Aug 28];37(10). Available from:
639 https://pubmed.ncbi.nlm.nih.gov/34879275/

640 44. Gudbjartsson DF, Sulem P, Stacey SN, Goldstein AM, Rafnar T, Sigurgeirsson B, et al.
641 ASIP and TYR pigmentation variants associate with cutaneous melanoma and basal cell
642 carcinoma. Nat Genet [Internet]. 2008 [cited 2024 Aug 28];40(7):886–91. Available from:
643 https://pubmed.ncbi.nlm.nih.gov/18488027/

644 45. Garraway LA, Widlund HR, Rubin MA, Getz G, Berger AJ, Ramaswamy S, et al.
645 Integrative genomic analyses identify MITF as a lineage survival oncogene amplified in
646 malignant melanoma. Nature [Internet]. 2005 Jul 7 [cited 2024 Aug 28];436(7047):117–
647 22. Available from: https://pubmed.ncbi.nlm.nih.gov/16001072/

648 46. Tassabehji M, Newton VE, Read AP. Waardenburg syndrome type 2 caused by
649 mutations in the human microphthalmia (MITF) gene. Nat Genet [Internet]. 1994 [cited
650 2024 Aug 28];8(3):251–5. Available from: https://pubmed.ncbi.nlm.nih.gov/7874167/

651 47. Bondurand N, Pingault V, Goerich DE, Lemort N, Sock E, Le Caignec C, et al. Interaction
652 among SOX10, PAX3 and MITF, three genes altered in Waardenburg syndrome. Hum
653 Mol Genet [Internet]. 2000 Aug 12 [cited 2024 Aug 28];9(13):1907–17. Available from:
654 https://pubmed.ncbi.nlm.nih.gov/10942418/

655 48. Paratore C, Eichenberger C, Suter U, Sommer L. Sox10 haploinsufficiency affects
656 maintenance of progenitor cells in a mouse model of Hirschsprung disease. Hum Mol
657 Genet [Internet]. 2002 Nov 15 [cited 2024 Aug 28];11(24):3075–85. Available from:
658 https://pubmed.ncbi.nlm.nih.gov/12417529/

659 49. Mccallion AS, Chakravarti A. EDNRB/EDN3 and Hirschsprung disease type II. Pigment
660 Cell Res [Internet]. 2001 [cited 2024 Aug 28];14(3):161–9. Available from:
661 https://pubmed.ncbi.nlm.nih.gov/11434563/

662 50. Sebag JA, Zhang C, Hinkle PM, Bradshaw AM, Cone RD. Developmental Control of the
663 Melanocortin-4 Receptor by MRAP2 Proteins in Zebrafish. Science [Internet]. 2013 Jul 7
664 [cited 2024 Jun 27];341(6143):278. Available from: /pmc/articles/PMC4255277/

665 51. Yeo GSH, Farooqi IS, Aminian S, Halsall DJ, Stanhope RG, O'Rahilly S. A frameshift
666 mutation in MC4R associated with dominantly inherited human obesity. Nat Genet
667 [Internet]. 1998 [cited 2024 Aug 28];20(2):111–2. Available from:
668 https://pubmed.ncbi.nlm.nih.gov/9771698/

669 52. Wade KH, Lam BYH, Melvin A, Pan W, Corbin LJ, Hughes DA, et al. Loss-of-function
670 mutations in the melanocortin 4 receptor in a UK birth cohort. Nat Med [Internet]. 2021
671 Jun 1 [cited 2024 Aug 28];27(6):1088–96. Available from:
672 https://pubmed.ncbi.nlm.nih.gov/34045736/

673 53. Amorim JP, Bordeira-Carriço R, Gali-Macedo A, Perrod C, Bessa J. CRISPR-Cas9-
674 Mediated Genomic Deletions Protocol in Zebrafish. STAR Protoc [Internet]. 2020 Dec 18
675 [cited 2023 Dec 20];1(3). Available from: https://pubmed.ncbi.nlm.nih.gov/33377102/

676 54. Jao LE, Wente SR, Chen W. Efficient multiplex biallelic zebrafish genome editing using a
677 CRISPR nuclease system. Proc Natl Acad Sci U S A [Internet]. 2013 [cited 2023 Dec
678 19];110(34):13904–9. Available from: https://pubmed.ncbi.nlm.nih.gov/23918387/

679 55. Kimmel CB, Ballard WW, Kimmel SR, Ullmann B, Schilling TF. Stages of embryonic
680 development of the zebrafish. Developmental Dynamics [Internet]. 1995 [cited 2025 Feb
681 9];203(3):253–310. Available from: https://pubmed.ncbi.nlm.nih.gov/8589427/

682 56. Schneider CA, Rasband WS, Eliceiri KW. NIH Image to ImageJ: 25 years of image
683 analysis. Nat Methods. 2012 Jul 28;9(7):671–5.

684 57. Siegenthaler A, Mondal D, Benvenuto C. Quantifying pigment cover to assess variation in
685 animal colouration. Biol Methods Protoc. 2017 Jan 1;2(1).

686 58. Cunningham RL, Kramer ET, DeGeorgia SK, Godoy PM, Zarov AP, Seneviratne S, et al.
687 Functional in vivo characterization of sox10 enhancers in neural crest and melanoma
688 development. Communications Biology 2021 4:1 [Internet]. 2021 Jun 7 [cited 2024 Aug
689 11];4(1):1–15. Available from: https://www.nature.com/articles/s42003-021-02211-0

690 59. Kawakami A, Fisher DE. The master role of microphthalmia-associated transcription
691 factor in melanocyte and melanoma biology. Laboratory Investigation 2017 97:6
692 [Internet]. 2017 Mar 6 [cited 2023 Aug 22];97(6):649–56. Available from:
693 https://www.nature.com/articles/labinvest20179

694 60. Cooper CD. Insights from zebrafish on human pigment cell disease and treatment.
695 Developmental Dynamics [Internet]. 2017 Nov 1 [cited 2024 Jul 31];246(11):889–96.
696 Available from: https://onlinelibrary.wiley.com/doi/full/10.1002/dvdy.24550

697 61. Moreno-Marmol T, Cavodeassi F, Bovolenta P. Setting eyes on the retinal pigment
698 epithelium. Front Cell Dev Biol [Internet]. 2018 Oct 24 [cited 2024 Jul 29];6(OCT):418922.
699 Available from: www.frontiersin.org

700 62. Baron M, Maillet J, Huyvaert M, Dechaume A, Boutry R, Loiselle H, et al. Loss-of-function
701 mutations in MRAP2 are pathogenic in hyperphagic obesity with hyperglycemia and
702 hypertension. Nature Medicine 2019 25:11 [Internet]. 2019 Nov 7 [cited 2024 Aug
703 13];25(11):1733–8. Available from: https://www.nature.com/articles/s41591-019-0622-0

704 63. Asai M, Ramachandrappa S, Joachim M, Shen Y, Zhang R, Nuthalapati N, et al. Loss of
705 function of the melanocortin 2 receptor accessory protein 2 is associated with mammalian
706 obesity. Science (1979) [Internet]. 2013 Jul 19 [cited 2024 Aug 13];341(6143):275–8.
707 Available from: https://www.science.org/doi/10.1126/science.1233000

708 64. Vaisse C, Clement K, Durand E, Hercberg S, Guy-Grand B, Froguel P. Melanocortin-4
709 receptor mutations are a frequent and heterogeneous cause of morbid obesity. J Clin
710 Invest [Internet]. 2000 [cited 2024 Aug 13];106(2):253–62. Available from:
711 https://pubmed.ncbi.nlm.nih.gov/10903341/

712 65. de Vrieze E, de Bruijn SE, Reurink J, Broekman S, van de Riet V, Aben M, et al. Efficient
713 generation of knock-in zebrafish models for inherited disorders using crispr-cas9
714 ribonucleoprotein complexes. Int J Mol Sci [Internet]. 2021 Sep 1 [cited 2023 Aug
715 22];22(17):9429. Available from: https://www.mdpi.com/1422-0067/22/17/9429/htm

716 66. Alerasool N, Segal D, Lee H, Taipale M. An efficient KRAB domain for CRISPRi
717 applications in human cells. Nature Methods 2020 17:11 [Internet]. 2020 Oct 5 [cited
718 2023 Nov 28];17(11):1093–6. Available from: https://www.nature.com/articles/s41592-
719 020-0966-x

720 FIG.URES

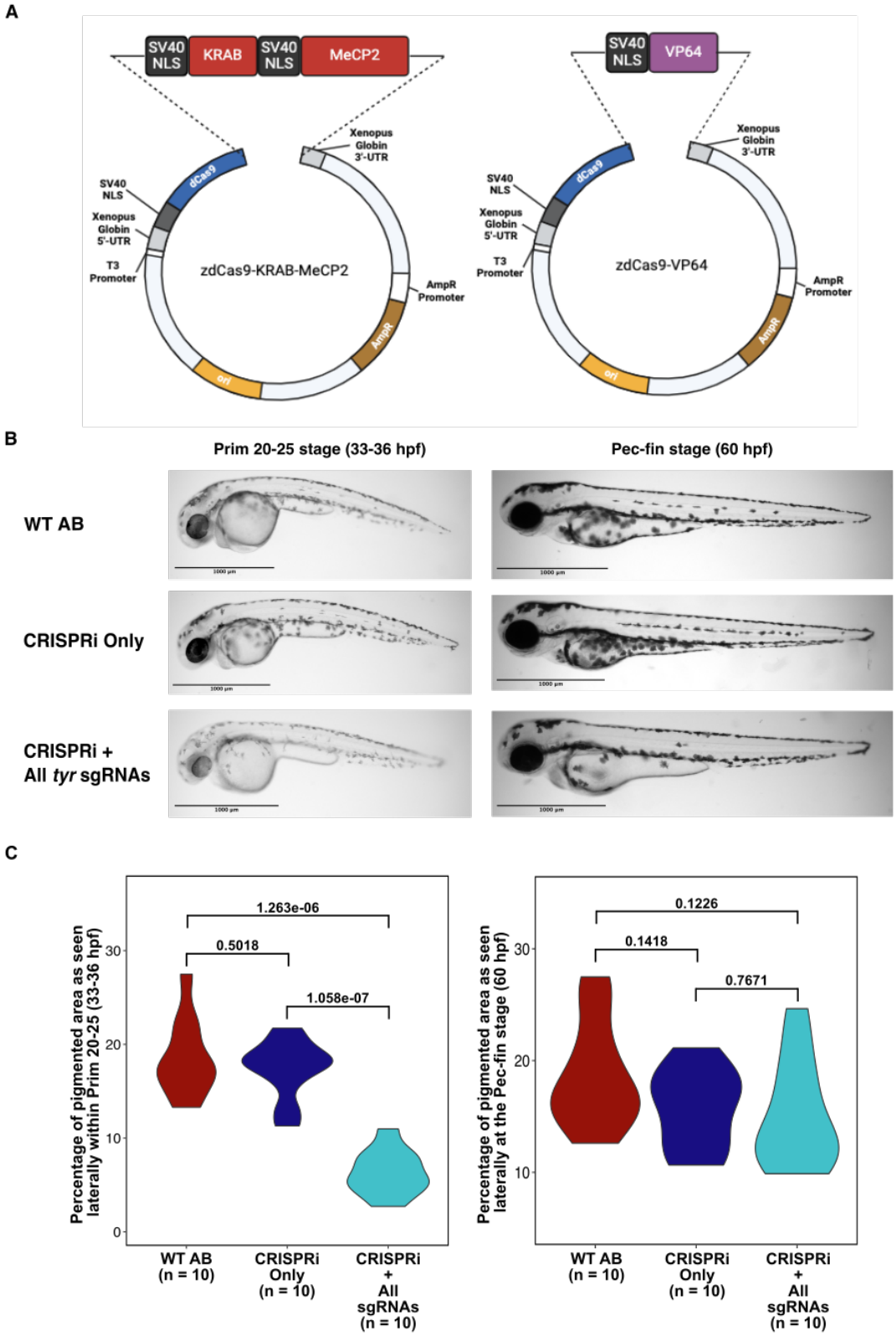

721

722 ***Figure 1:*** CRISPRi/a construct design and *tyr* silencing. **A.** Zebrafish codon-optimized plasmids were
723 synthesized using NEB HiFi DNA assembly, transformed and amplified in NEB 5-α chemically competent
724 cells. Plasmid DNA was linearized and *in vitro* transcribed before microinjection into one-cell embryos. **B.**
725 Zebrafish embryos injected with CRISPRi (final concentration 100-300 ng/µl) + cocktail of sgRNAs (final
726 concentration 150 ng/µl) targeting *tyr* assayed at prim 20-25 (33-36 hpf) and pec-fin (60 hpf) stages for
727 differences in pigmentation patterns. The larvae injected with CRISPRi and sgRNAs displayed reduced
728 pigmentation at the prim 20-25 stage when compared to controls. The effect of CRISPRi dissipated by the
729 pec-fin stage as observable pigmentation patterns were indistinguishable. Scale bars 1000 µm. **C.** Pigment
730 analysis of larvae at Prim 20-25 stage (33-36 hpf) and Pec-fin stage (60 hpf) to measure the percentage of
731 pigmented area, as viewed laterally. At Prim 20-25, the percentage of pigmented area is statistically
732 significant (Welch two-sample t-test); by contrast, at Pec-fin, while not statistically significant,
733 CRISPRi+sgRNA injected embryos show less percentage of pigmented area than WT AB and injection
734 controls.

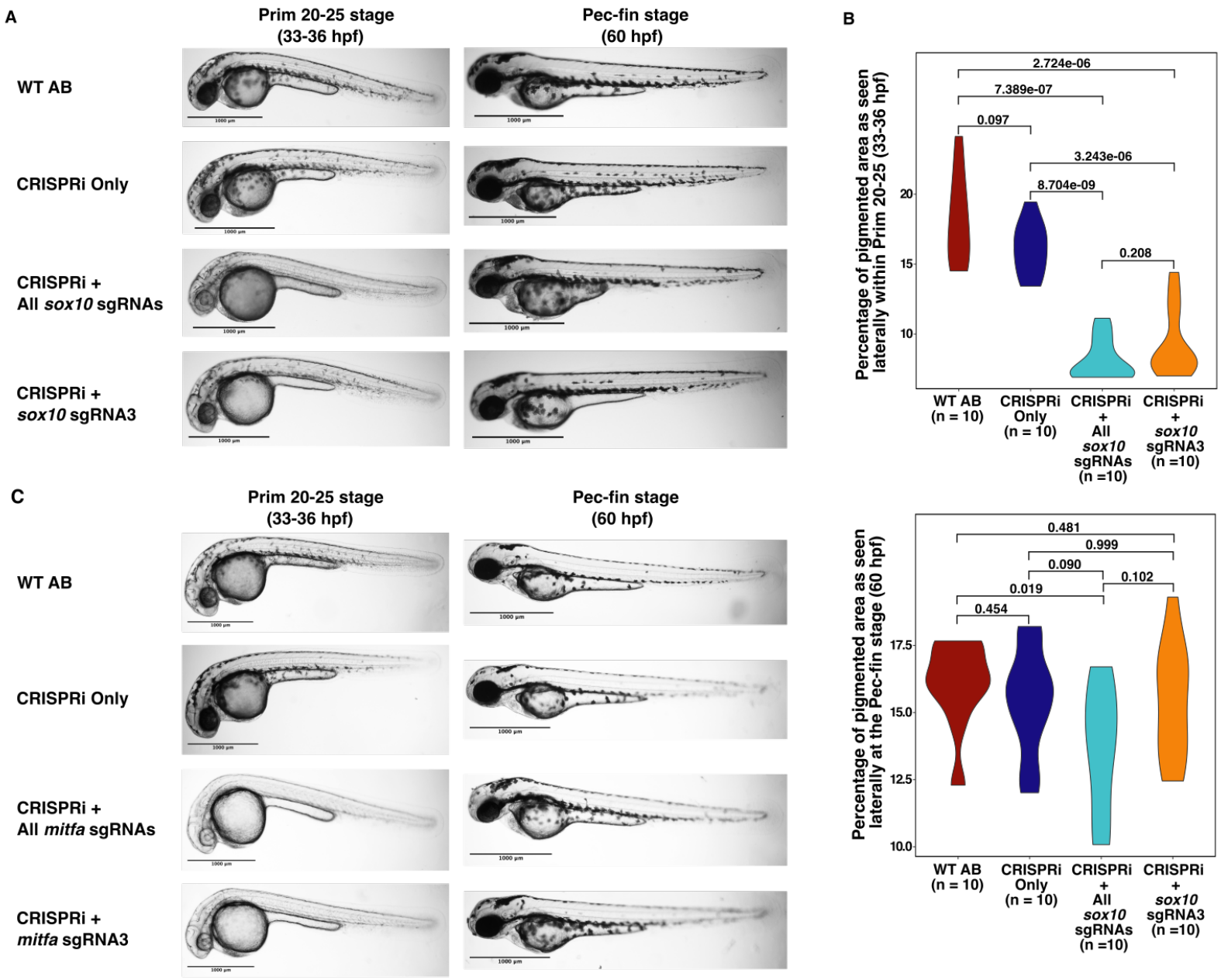
A
Prim 20-25 stage
(33-36 hpf)
Pec-fin stage
(60 hpf)
WT AB
CRISPRi Only
CRISPRi +
All sox10 sgRNAs
CRISPRi +
sox10 sgRNA3
B
Percentage of pigmented area as seen laterally within Prim 20-25 (33-36 hpf)
2.724e-06
7.389e-07
0.097
3.243e-06
8.704e-09
0.208
20
15
10
WT AB (n = 10)
CRISPRi Only (n = 10)
CRISPRi + All sox10 sgRNAs (n =10)
CRISPRi + sox10 sgRNA3 (n =10)
C
Prim 20-25 stage
(33-36 hpf)
Pec-fin stage
(60 hpf)
WT AB
CRISPRi Only
CRISPRi +
All mitfa sgRNAs
CRISPRi +
mitfa sgRNA3
Percentage of pigmented area as seen laterally at the Pec-fin stage (60 hpf)
0.481
0.999
0.090
0.102
0.019
0.454
17.5
15.0
12.5
10.0
WT AB (n = 10)
CRISPRi Only (n = 10)
CRISPRi + All sox10 sgRNAs (n =10)
CRISPRi + sox10 sgRNA3 (n =10)

735

736 ***Figure 2:*** CRISPRi targeting the promoters of the *sox10* and *mitfa* genes. **A.** Zebrafish 1-cell embryos injected with CRISPRi + sgRNAs targeting
737 *sox10* assayed at prim 20-25 (33-36 hpf) and pec-fin (60 hpf) stages for differences in pigmentation patterns. WT AB and injected controls did not
738 show reduced pigmentation around the prim 20-25 stages, whereas embryos injected with CRISPRi + All *sox10* sgRNAs or CRISPRi + *sox10*
739 sgRNA3 were hypopigmented. **B.** At the prim 20-25 stage, differences in pigmentation patterns across conditions are statistically significant (*p-*
740 *value* < 0.05). At the pec-fin stage, the effect of CRISPRi dissipated as patterns of hypopigmentation are less variable with the only statistically
741 significant difference being between WT AB and CRISPRi + All *sox10* sgRNAs based on Welch two-sample t-test. **C.** Zebrafish embryos injected
742 with CRISPRi + sgRNAs targeting the *mitfa* promoter. Larvae were assayed at prim 20-25 and pec-fin stages for differences in pigmentation
743 patterns. At this stage, embryos injected with CRISPRi + All sgRNAs or CRISPRi + sgRNA3 displayed a hypopigmented pattern as compared to
744 injected and uninjected controls. At the pec-fin stage, the effect of CRISPRi has dissipated as patterns of hypopigmentation displayed no
745 significant differences across conditions. Scale bars: 1000 μm.

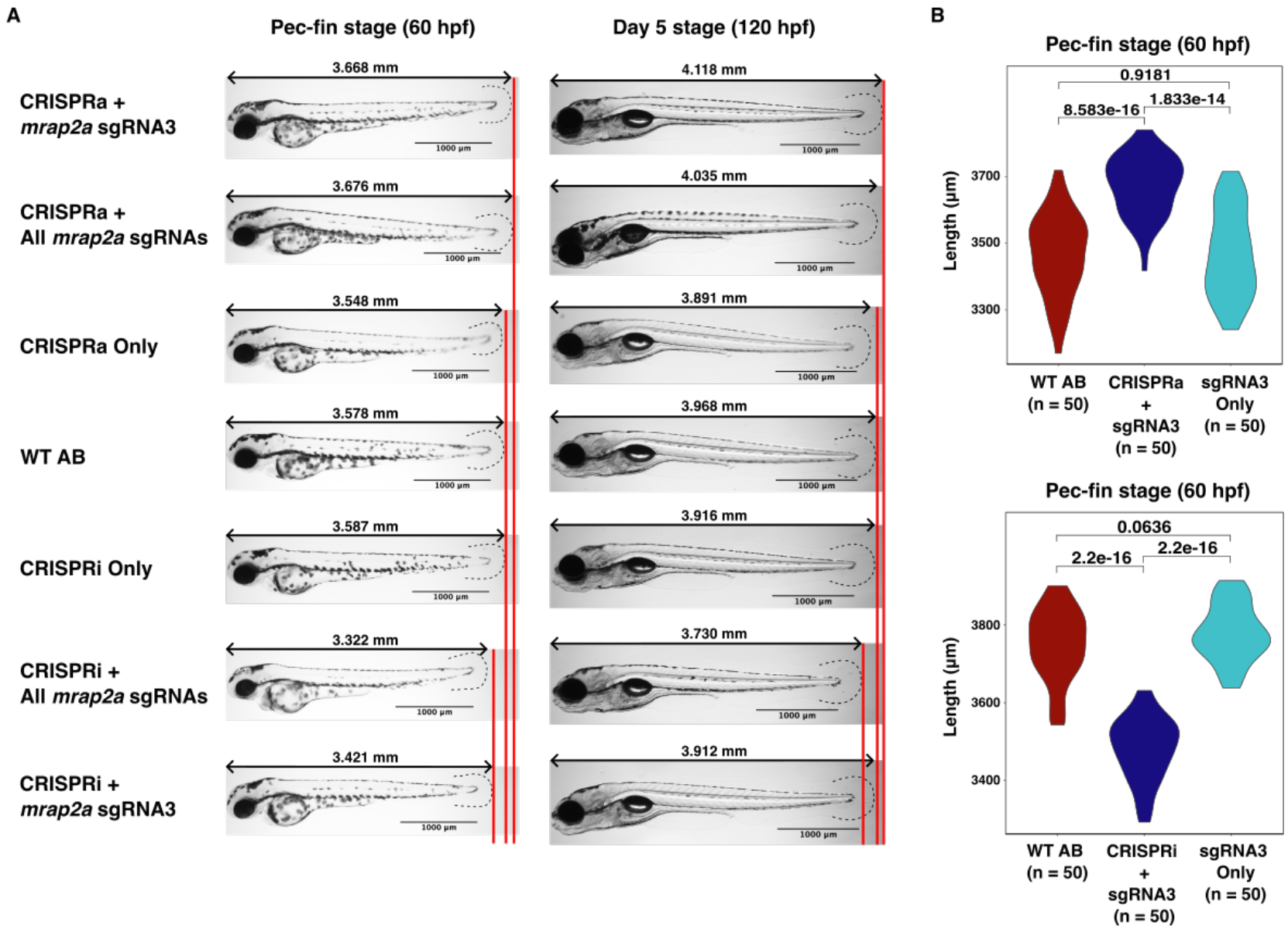
A
Pec-fin stage (60 hpf)
Day 5 stage (120 hpf)
CRISPRa + mrap2a sgRNA3
3.668 mm
4.118 mm
CRISPRa + All mrap2a sgRNAs
3.676 mm
4.035 mm
CRISPRa Only
3.548 mm
3.891 mm
WT AB
3.578 mm
3.968 mm
CRISPRi Only
3.587 mm
3.916 mm
CRISPRi + All mrap2a sgRNAs
3.322 mm
3.730 mm
CRISPRi + mrap2a sgRNA3
3.421 mm
3.912 mm
1000 µm
B
Pec-fin stage (60 hpf)
0.9181
8.583e-16
1.833e-14
Length (µm)
3700
3500
3300
WT AB (n = 50)
CRISPRa + sgRNA3 (n = 50)
sgRNA3 Only (n = 50)
Pec-fin stage (60 hpf)
0.0636
2.2e-16
2.2e-16
Length (µm)
3800
3600
3400
WT AB (n = 50)
CRISPRi + sgRNA3 (n = 50)
sgRNA3 Only (n = 50)

746

747 ***Figure 3:*** Targeting the promoter of *mrap2a* with CRISPRa and CRISPRi. **A.** Length comparison between the pec-fin and day-5 stages between
748 WT AB embryos and embryos injected with CRISPRa and CRISPRi with all *mrap2a* sgRNAs or only sgRNA3. Length measured laterally from tip
749 of the mouth to end of translucent tail fin (dashed lines). Red lines depict length differences between controls and experimental conditions. Scale
750 bars: 1000 μm. **B.** At the pec-fin stage, 50 larvae per condition were measured in length from the tip of the mouth to the end of the translucent tail
751 fin. The Welch two-sample t-test was used to compare the average length between conditions.

750 SUPPLEMENTAL FIG.URES

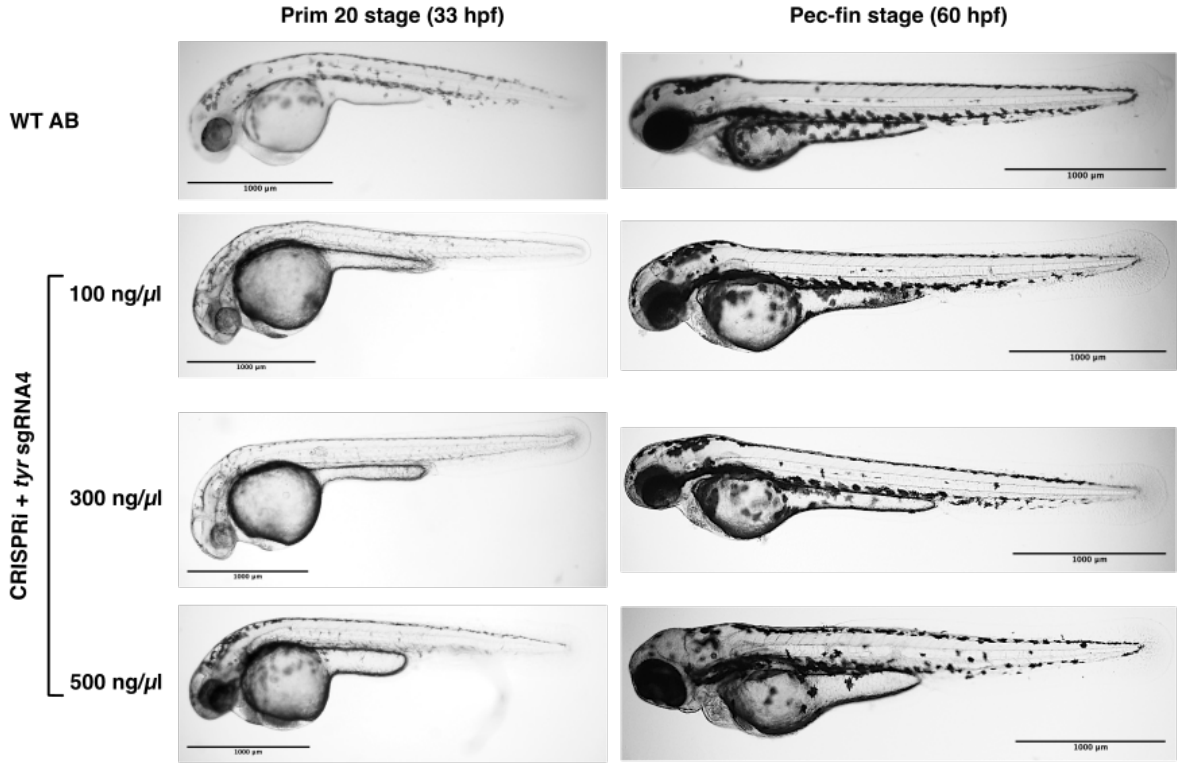

751

752 ***Supplemental Figure 1:*** Assessment of optimal mRNA concentration for injection

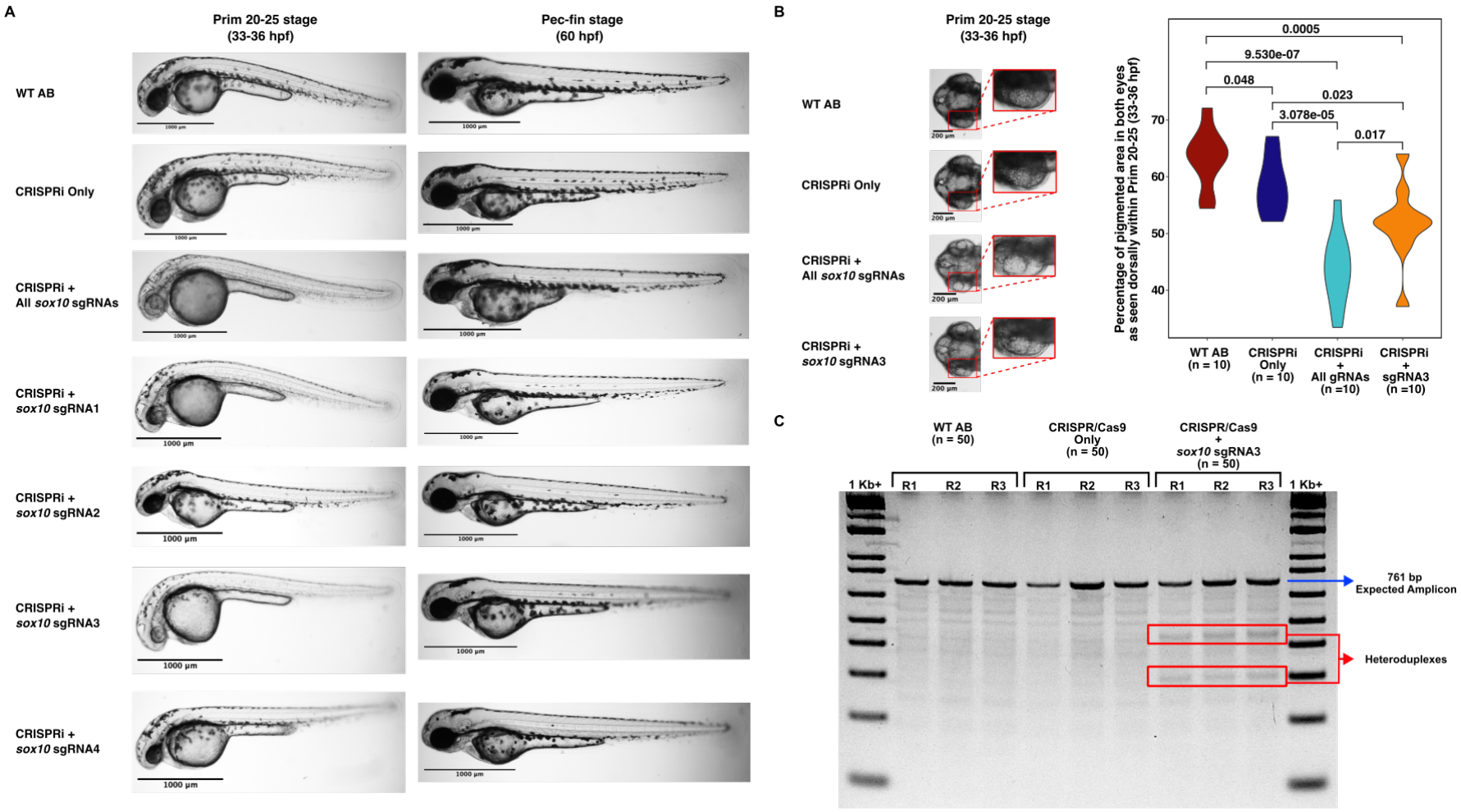

Supplemental Figure 2: Targeting the *sox10* promoter with CRISPRi. **A.** Larvae at prim 20-25 (33-36 hpf) and pec-fin (60 hpf) stages across conditions. Scale bars 1000 µm. **B.** At the prim 20-25 stage, RPE pigmentation is variable across conditions; however, differences are statistically significant between controls and injected conditions. **C.** Gel (2% agarose) electrophoresis of T7 endonuclease I assay to detect heteroduplex formation (red boxes) after targeting the *sox10* promoter with sgRNA3. Expected amplicon length is 761 bp (blue arrow).

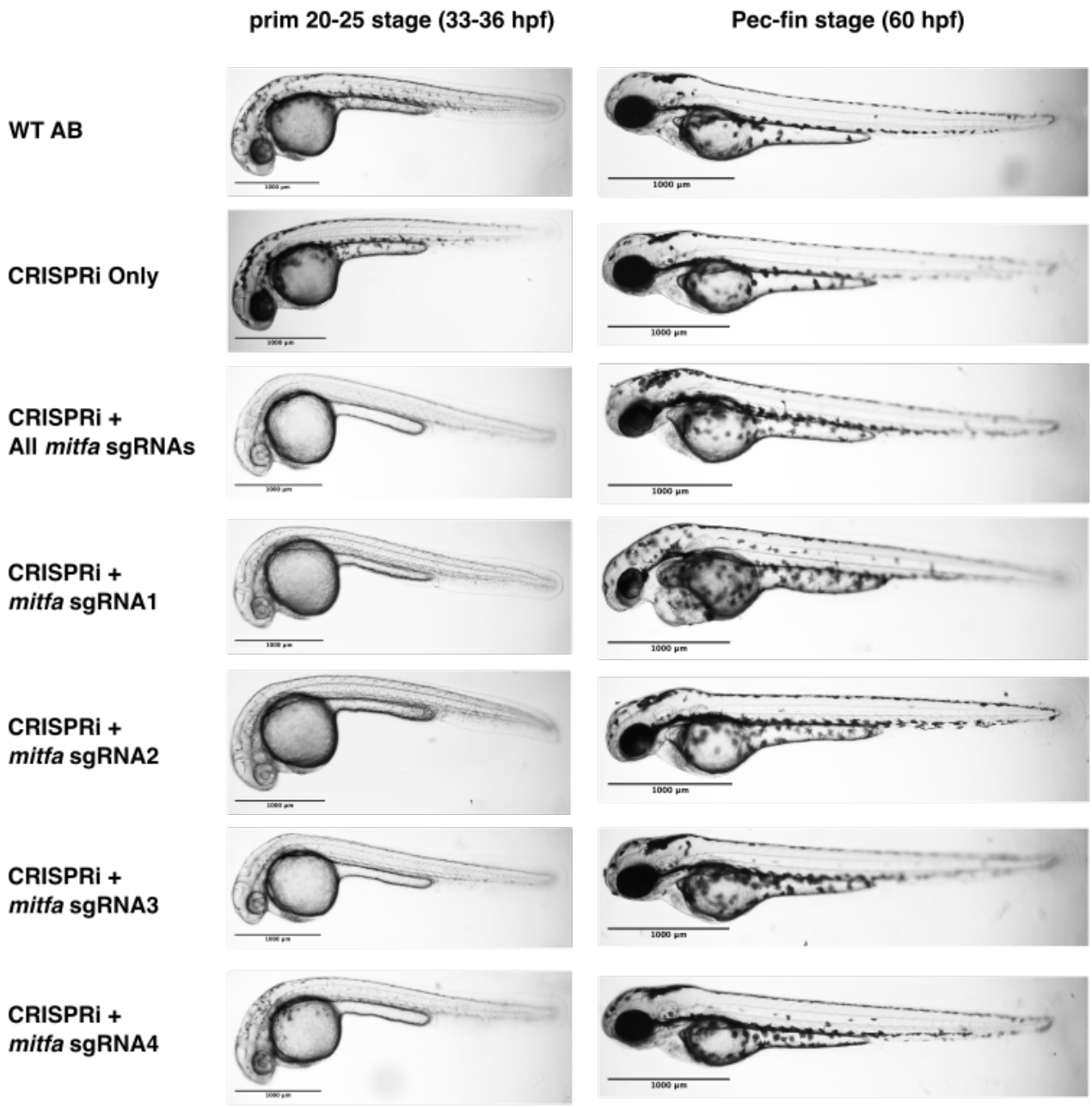

758
759 ***Supplemental Figure 3:*** Targeting the *mitfa* promoter with CRISPRi. Scale bars 1000 µm.

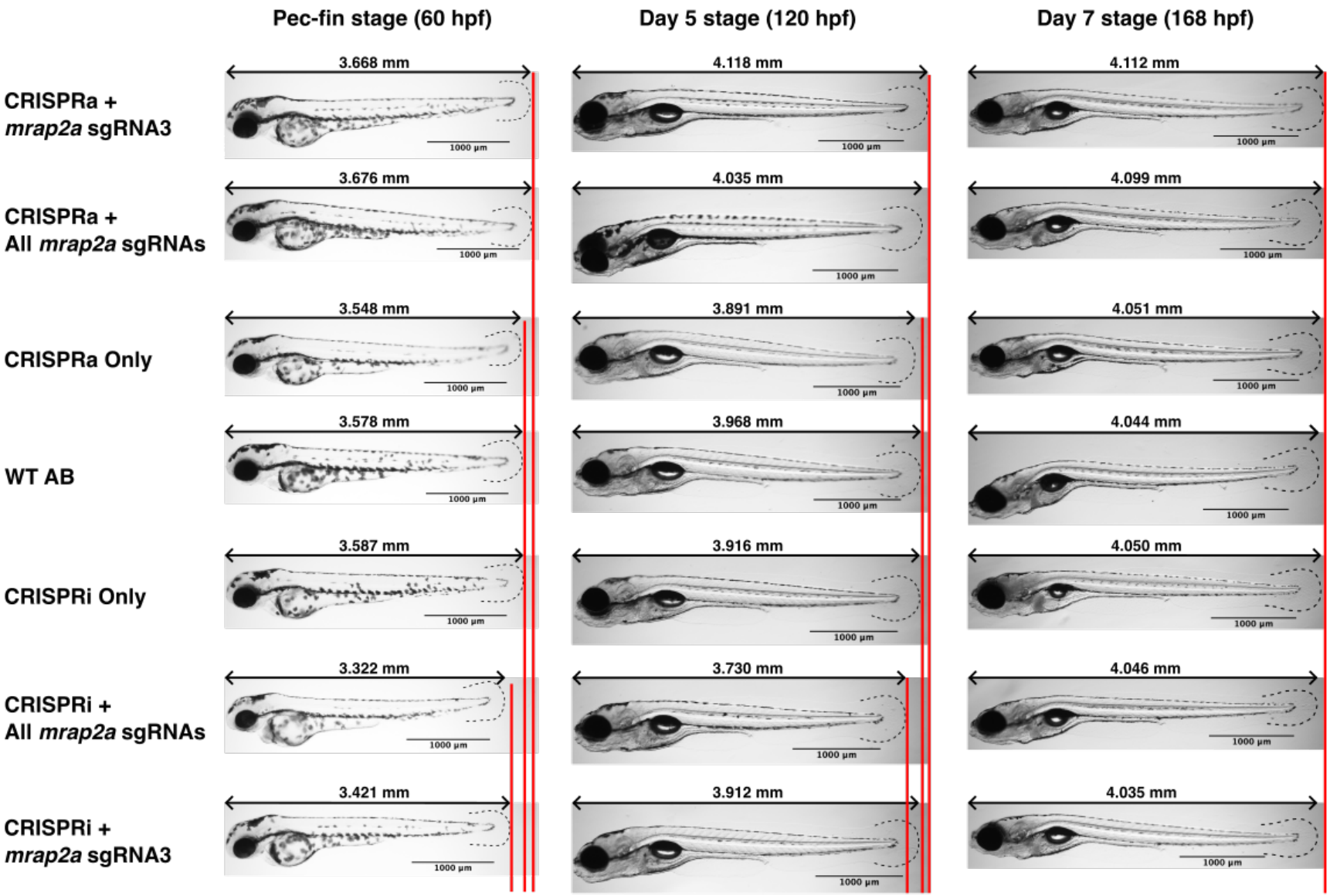
Pec-fin stage (60 hpf)
Day 5 stage (120 hpf)
Day 7 stage (168 hpf)
CRISPRa + mrap2a sgRNA3
3.668 mm
4.118 mm
4.112 mm
CRISPRa + All mrap2a sgRNAs
3.676 mm
4.035 mm
4.099 mm
CRISPRa Only
3.548 mm
3.891 mm
4.051 mm
WT AB
3.578 mm
3.968 mm
4.044 mm
CRISPRi Only
3.587 mm
3.916 mm
4.050 mm
CRISPRi + All mrap2a sgRNAs
3.322 mm
3.730 mm
4.046 mm
CRISPRi + mrap2a sgRNA3
3.421 mm
3.912 mm
4.035 mm
1000 µm

760

761 ***Supplemental Figure 4:*** CRISPRa and CRISPRi targeting of the mrap2a promoter. Images taken at pec-fin, day 5, and day 7 stages. Dotted lines
762 represent the translucent tail fin of the larvae. Scale bars 1000 μm.